



Article

Multi-AUV Kinematic Task Assignment based on Self-organizing Map Neural Network and Dubins Path Generator

Xin Li ^{1,*}, Wenyang Gan ², Pang Wen ³ and Daqi Zhu ³

¹ College of Information Engineering, Shanghai Maritime University, Shanghai 201306, China

² Logistics Engineering College, Shanghai Maritime University, Shanghai 201306, China

³ Mechanics Institute, University of Shanghai for Science and Technology, Shanghai 200093, China

* Correspondence: xinli@shmtu.edu.cn; lixin850224@163.com

† Current address: 1550 Haigang Avenue, Pudong New Area, Shanghai, China.

Abstract: To deal with the task assignment problem of multi-AUV systems under kinematic constraints, which means steering capability constraints for underactuated AUVs or other vehicles likely, an improved task assignment algorithm is proposed combining the Dubins Path algorithm with improved SOM neural network algorithm. At first, the aimed tasks are assigned to the AUVs by improved SOM neural network method based on workload balance and neighborhood function. When there exists kinematic constraints or obstacles which may cause failure of trajectory planning, task re-assignment will be implemented by change the weights of SOM neurals, until the AUVs can have paths to reach all the targets. Then, the Dubins paths are generated in several limited cases. AUV's yaw angle is limited, which result in new assignments to the targets. Computation flow is designed so that the algorithm in MATLAB and Python can realizes the path planning to multiple targets. Finally, simulation results prove that the proposed algorithm can effectively accomplish the task assignment task for multi-AUV system.

Keywords: multi-AUV; task assignment; kinematic constraints; Dubins path; SOM Neural Network

0. Introduction

At present time, there have been a lot of theoretical and practical research results on the task assignment algorithms for multi-AUV system. The task assignment algorithm covers two aspects: 1. task allocation and 2. path planning, which refers to the technology of controlling a group of AUVs according to a certain algorithm and reaching the target along the optimized path under the kinematic constraints. In other words, task allocation ensures optimized task assignment such as Traveling Salesman Problem (TSP); path planning guarantees the feasibility for the agents moving to the assigned tasks. For underwater vehicles, task assignment refers to the assignment of a number of targets to a multi-AUV system, and the cost of the whole multi-AUV system is minimum under the premise that all targets are traversed. Path planning technique refers to the achievement method for any single AUV in the group after global task assignment [1].

The market mechanism algorithm is one the most common method to solve the multitask assignment operations [2]. Another commonly used task assignment algorithm is ant colony algorithm which mainly studies the autonomous task assignment of multi-robot systems in dynamic environments [3]. These are also other task assignment methods, such as that with intelligent heuristic algorithm handling water flow influence [4], while kinematic path planning not considered for most of them. As for neural networks, literature [5] further proposed a task allocation algorithm suitable for large-scale multi-robot clusters. The self-organizing neural network algorithm can also be applied to multi-task assignment. The SOM algorithm was proposed by a Finnish scholar, Teuvo Kohonen, in the 1980s [6,7].

arXiv:2405.07536v4 [cs.RO] 13 Jun 2024



Citation: Li, X.; Gan, W.; Pang, W.; Zhu, D. Multi-AUV Kinematic Task Assignment based on Self-organizing Map Neural Network and Dubins Path Generator. *Sensors* **2024**, *1*, 0. <https://doi.org/>

Received:
Revised:
Accepted:
Published:



Copyright: © 2024 by the authors. Licensee MDPI, Basel, Switzerland. This article is an open access article distributed under the terms and conditions of the Creative Commons Attribution (CC BY) license (<https://creativecommons.org/licenses/by/4.0/>).

Literature [8,9] applied the self-organizing neural network to the task assignment and distribution of multi-mobile robot systems. path planning. Using the SOM neural network algorithm, dynamic task assignments for multi-AUV systems in two-dimensional ocean environments are implemented. Then, the multi-AUV multi-target allocation strategy of self-organizing map (SOM) neural network is further extended and applied to the three-dimensional marine environment [10]. Event-triggered adaptive neural network tracking control for uncertain systems was proposed in [11], where the event-triggering mechanism can reduce the update rate of input signals and avoid the Zeno behavior.

Path planning is one of the intelligent behaviors that AUVs need to possess. The so-called path planning means that in an environment with obstacles, the AUV finds a collision-free path from the initial state to the target state according to certain evaluation criteria [12,13]. Traditional path planning methods mainly include: visual graph method, artificial potential field method, genetic algorithm, fuzzy logic method, etc [14–16]. These path planning methods have their own scope of application. However, underwater movements of the AUVs have limitations. If the steering performance by the rudder is limited, with the maximum angle of steering θ , the maximum turning radius should be R . For this reason, the minimum turning radius should not be less than R , which put constraints on the movements. Most of the traditional path planning methods did not consider the kinematic constraints. In another situation, a configurable maximum pitch angle γ is set to control the behaviour of the climbing of the AUV. In case the necessary pitch angle between two waypoints exceeds this angle, a helical path is introduced to avoid the generation of pitch set-points that might make the vehicle stall. The Dubins path planning method can handle these two kind of situations caused by the vehicle kinematic constraints [17,18]. The Dubins method is mainly based on the following theorem. When the direction of motion is known and the turning radius is the smallest, the shortest path from the initial vector to the ending vector is composed of a straight line and a turning arc with the smallest radius. AUV can effectively save energy by using the shortest path in task assignment and path planning. Although the problem of multi-task assignment has been extensively studied, none of the literature mentioned above considered AUV's underwater kinematic constraints. This issue has certainly been studied before by some scholars from different perspectives, but overall the research is relatively rare. The AUV underwater task assignment and path planning in the actual environment cannot ignore the kinematic constraints and the actual existence of the obstacle environment. This paper mainly conducts in-depth research on this.

As shown in Figure 1, a typical AUV has 1-2 thrusters at the tail, relying on rudder and fins to control the moving direction. This structure determines that most AUVs are underactuated. When an AUV moves, it turns horizontally and tilts vertically, i.e., yaw and pitch. The yaw and pitch angles are limited due to mechanical structure and fluid dynamics. In 3D workspace, pitch angle $\gamma \leq \gamma_{max}$, and yaw angle's derivative or the angular velocity on X-Y plane $\dot{\phi}$ is also limited, which results the turning radius $r \geq R$, where R is the minimum turning radius under the angular velocity $max(\dot{\phi})$. It should be noted that when the force of the thruster is set very high, the turning radius will also be large at the maximum rudder angle, while we are discussing the case of normal thrust. Considering this, task assignment and path planning of multiple AUV systems under kinematic constraints in a two-dimensional environment are studied in this paper, taking into account static obstacles and other interference factors. The main innovation is to combine the task assignment of SOM neural networks with Dubins path planning under kinematic constraints, making the method more applicable to real-world applications. By combining the Dubins Path algorithm with the improved self-organizing mapping (SOM) neural network algorithm, this paper proposes a new task assignment and path planning algorithm, which effectively solves the multi-task assignment problem of the multi-AUV system in the actual environment. The mathematical model and algorithms are established on MATLAB, and then tested in Python on a Raspberry Pi.

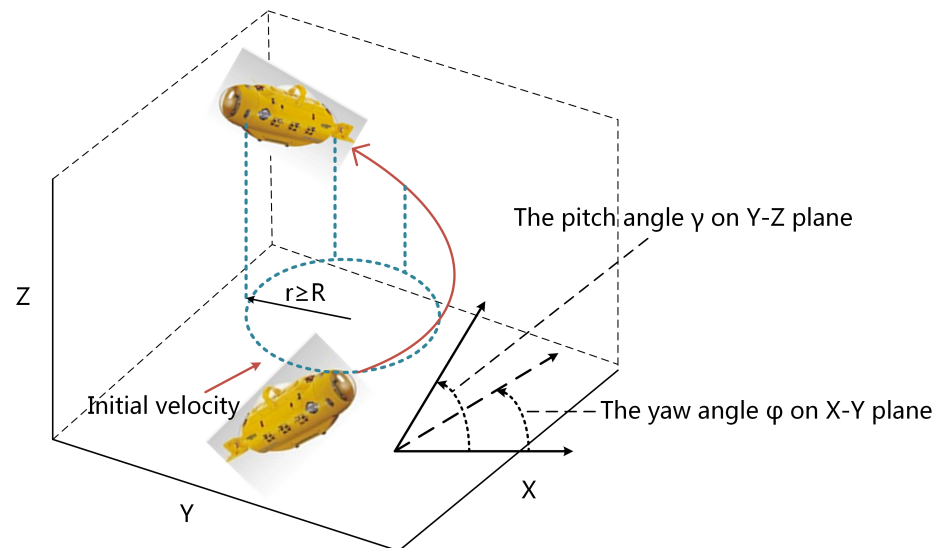


Figure 1. AUV's kinematic constraint in 3D workspace.

This paper is organized as follows. A hierarchical controller structure is proposed for MAS formation control in Section II. The AUVs' kinematics and dynamics are represented in the specific reference frames in section III, where the water flow models are established as well. In Section IV, we introduce the adaptive sliding mode control method and set the propeller configuration for simulations. In section V, simulation results are presented for formation control of a group of AUVs in the 3-D environment. Some conclusive remarks are given in Section VI.

1. Problem Formulation

The task allocation algorithm of a multi AUV system covers two aspects: task allocation and path planning, which refer to the technology of controlling a group of AUVs based on a certain algorithm, and each of them reaches the target along the optimized path under kinematic constraints.

Task allocation refers to assigning any number of targets to a group of underwater robots, ensuring that all targets are traversed while minimizing the cost of the entire multi AUV system, i.e. minimizing the total walking distance. Path planning technology refers to a path planning method for a single AUV after global task allocation. This article mainly focuses on the task allocation and path planning problem of multi AUV systems under kinematic constraints in two-dimensional and three-dimensional environments, and considers interference factors such as obstacles. A 3D visual example is provided in Figure 2.

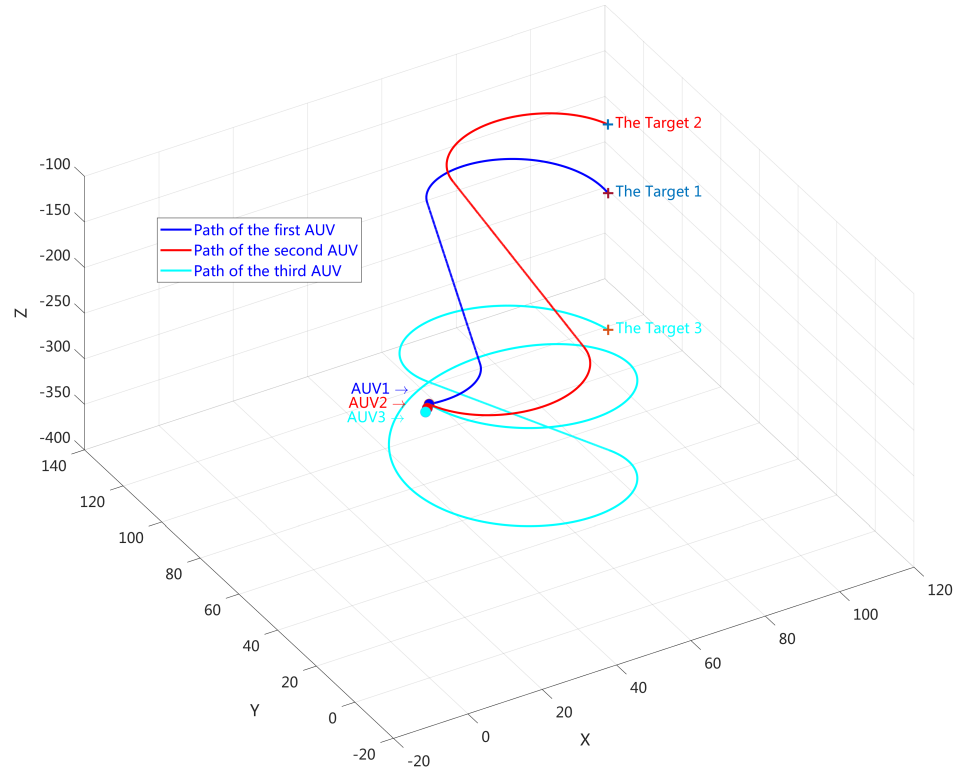


Figure 2. An example of Multi-AUV task assignment: 3 AUVs and 3 targets.

Relying solely on the principle of proximity between target point coordinates and AUV coordinates to allocate tasks may sometimes result in one AUV being assigned too many tasks, making it unable to fully reach all assigned targets before running out of power, while other AUVs may not be able to achieve the task objectives. The initially assigned tasks cannot be completed in the actual planned path due to obstacles. In order to ensure the maximum utilization of energy carried by each AUV and avoid the AUV stopping due to insufficient energy during its movement towards the target, load balancing of the AUV should be considered.

Assuming that AUVs have the same underwater cruising capability, carrying the same energy, the maximum number of each AUV should be decided firstly. Note that we do not consider the energy consumption difference caused by the turning radius for now, only the distance traveled. Firstly, calculate $N = N_T / N_R$, where N_T is the number of target points and N_R is the number of AUVs, then set the upper limit of the task load to

$$N_{MAX} = \begin{cases} N, & N \in N^+ \\ \lfloor N \rfloor + 1, & N \notin N^+ \end{cases} \quad (1)$$

When the maximum number of tasks is exceeded the certain number for an AUV, the task will not be assigned to it again, and the suboptimal AUV will be selected to execute the task. Considering the load balancing of AUV systems into the algorithm is an important improvement, making them more suitable for the actual situation of multi AUV and multi task allocation. Meanwhile, we consider this problem in reverse and sequentially select the optimal target point for the AUV until the number of tasks for the AUV approaches N_{MAX} . At this point, we then calculate the energy loss of a single AUV to ultimately complete the task allocation.

After the optimal task assignment, path planning must be implemented with consideration of the kinematic constraints. Assuming that the AUV's initial and final poses are denoted by $P_g(x_g, y_g, z_g, \varphi_g, \gamma_g)$ and $P_g(x_g, y_g, z_g, \varphi_g, \gamma_g)$ respectively, where φ_i, γ_i represent the heading and pitch angles, respectively [19,20]. In the Cartesian coordinate frame

(x, y, z) , the path connecting the two poses is provided by trajectory smoothing, which can be written as

$$\begin{cases} \frac{dx}{ds} = \cos \varphi(s) \cos \gamma(s) \\ \frac{dy}{ds} = \sin \varphi(s) \cos \gamma(s) \\ \frac{dz}{ds} = \sin \gamma(s) \\ \frac{d\varphi}{ds} = \mu_1 \\ \frac{d\gamma}{ds} = \mu_2 \end{cases} \quad (2)$$

where s represents the curvilinear abscissa along the path, μ_1 and μ_2 represent the control inputs. The curvature radius $R(s)$ is calculated as follows:

$$R(s) = \frac{1}{\sqrt{\mu_1^2(s) \cos^2 \gamma(s) + \mu_2^2(s)}} \quad (3)$$

As there are certain relationships between geometric constraints and the vehicle actual constraints, control inputs (μ_1, μ_2) should be determined to satisfy these geometric constraints: (1) the curvature radius constraint: $|R| \geq R_{min}$; (2) the pitch angle constraint: $\gamma_{min} \leq \gamma \leq \gamma_{max}$. Essentially, finding the shortest path is an optimal control problem. For a group of AUVs, we are trying to find the optimal total consumption of all AUVs after completing their tasks described as

$$\sum_1^N \min \int_0^{s_{gn}} ds \quad (4)$$

where s_{gn} represents the planned trajectory length of the n th AUV.

In this paper, Dubins path is used to handle this issue. In this way, we can plan executable formation trajectories. It should be noted that the energy loss and formation task reassignment caused by different servo angles of the AUVs are not currently within the scope of this article.

2. Task assignment algorithm under kinematic constraints

In this section, self-organizing map (SOM) neural network method with Dubins path generator is used to deal with task allocation and path planning problems for the multi-AUV system. The control stability and accuracy of the system model are compensated by strengthening the optimal global exploration and local exploitation ability. **At the same time, an event-triggered neural network evolution strategy is developed to decrease the update frequency of the control signal. The improved optimization method can realize the controller's online parameter adjustment to meet the AUVs' control requirements in the experimental simulation environment.**

2.1. Application of *Event-triggered* SOM in Multi-AUV Task Assignment

Assuming a group of AUVs is distributed within a limited working area, and a random number of targets are distributed within this area. Each target point requires one AUV to complete a specific task at that point. For each AUV, its cost is measured by the distance it moves from the starting position coordinate point to the target position coordinate point. The total cost is defined as the sum of all individual AUV costs. After all target points have been visited once, the task is completed.

For the sake of simplicity, a two-dimensional plane is used as the workspace, in which the red points represent the AUV and the green circles represent the target point. Furthermore, assuming that all AUVs are the same robots with basic navigation, obstacle avoidance, and position recognition functions. For an input neuron (target point), the output neuron competes to become the winning neuron, as follows:

$$[N_j, N_l] = \min \left\{ D_{kjl}, k = 1, \dots, K; j = 1, \dots, J; l = 1, \dots, L \right\} \quad (5)$$

where $[\mathbf{N}_j, \mathbf{N}_l]$ represents the \mathbf{N}_j th output neuron that competes to win against the \mathbf{N}_l th input neuron in the k th iteration. D_{kjl} is a weight related variable according to relative distance, defined as:

$$D_{kjl} = \begin{cases} |\mathbf{T}_l - \mathbf{R}_{jk}|(1 + V), & P_j < S_{\max} \\ \infty, & P_j \geq S_{\max} \end{cases} \quad (6)$$

where S_{\max} is the maximal distance that a single AUV can travel, and

$$|\mathbf{T}_l - \mathbf{R}_{jk}| = \sqrt{(x_l - w_{jkx})^2 + (y_l - w_{jky})^2}. \quad (7)$$

Equation (7) provides an expression for finding the Euclidean distance between the target location \mathbf{T}_l and the AUV location \mathbf{R}_{jk} ; specifically, $\mathbf{T}_l = (T_{lx}, T_{lv})$ is the coordinate of the input neuron in the Cartesian coordinate system; $\mathbf{R}_{jk} = (w_{jkx}, w_{jky})$ ($k = 1, 2, \dots, K; j = 1, 2, \dots, J$) is the coordinate of the k th neuron in the j th output neuron group, which is the position of a specific AUV at a certain moment. The parameter V is given by (8), which controls the load balancing between various AUVs. The load balance function is the core of the SOM algorithm. The winning neuron in competition is not only the neuron with the smallest Euclidean distance from the input neuron, but also the neuron with the smallest load at that moment.

$$V = \frac{P_j - \bar{v}}{1 + \bar{v}} \quad (8)$$

where P_j is the path length of the j th AUV's movement, and \bar{v} is the average path length of the AUV team.

After a AUV's representing neuron wins the competition, a neighborhood function is an important step. The neighborhood function determines the influence (attraction strength) of the input neuron on the winning neuron and its adjacent neurons. The impact on the winning neuron should be the greatest. The impact on neighboring neurons gradually decreases, while neurons outside the neighboring area are not affected. The magnitude of the impact determines the size of the weight adjustment of neurons in the neighborhood during a certain iteration process. The process of calculating neighborhood functions and changing weights is shown in Figure 3. The red dots represent the position of the AUV at a certain moment, serving as output layer neurons; The green circle represents the target position as the input neuron. The winning neuron in the figure is R_1 , which is one closest to the input T_1 . The neighborhood function is defined as:

$$f(d_j, G) = \begin{cases} e^{-d_j^2/G^2(t)}, & d_j < r \\ 0, & \text{other} \end{cases} \quad (9)$$

It is easy to see that $0 \leq f(d_j, G) \leq 1$, where $d_j = \|\mathbf{j} - \mathbf{N}_l\|$, representing the distance between the j th neuron in the k th group and the winning neuron \mathbf{N}_l . r is the neighborhood radius. $G(t) = (1 - m)^t G_0$, where t is the number of iterations. When t increases, the value of the neighborhood function decreases, and the moving step of the AUV in the neighborhood decreases. m and G_0 are constants, through which the motion step size of AUVs in the neighborhood can be adjusted, thereby controlling calculation accuracy and operation time.

After the winning neuron and its neighborhood are determined, the winning neuron and adjacent neurons move towards the input neuron, while the other neurons remain stationary. The update rule is given by (10), where the addition operator represents vector addition. The termination condition for the operation is provided by D_{\min} , which can reduce the calculation time. The modification of weight values depends not only on the

initial distance between the winning neuron and its neighboring neurons and the input target point, but also on the neighborhood function and the learning rate of the network α .

$$\mathbf{R}_{jk}(t+1) = \begin{cases} \mathbf{T}_l(t), & D_{kjl} < D_{\min} \\ \mathbf{R}_{jk}(t) + \alpha \cdot f(d_j, G) \cdot (\mathbf{T}_l(t) - \mathbf{R}_{km}(t)), & \text{other} \end{cases} \quad (10)$$

At the same time, if there exists an obstacle at the position $ob = (x_o, y_o)$, the obstacle weight is computed based on the Euclidean distance between it and the neural network weights by

$$ob_w = \min(|\mathbf{ob} - \mathbf{R}_{jk}|) \quad (11)$$

where \mathbf{ob} is the expansion of ob to a vector of equal length to \mathbf{R}_{jk} ($j = 1, 2, \dots, J; k = 1, 2, \dots, K$). By comparing ob_w with the defined safety distance d_{safety} , the impact of obstacles can be determined.

The flowchart of the algorithm is shown in Figures 4. After initializing the SOM neural network, the positions of the target points are sequentially input into the network. For a given input target point during the iteration process, it can be summarized as a three-step calculation process. The first step is to select the winning neuron; the second step is to determine the neighborhood of the winning neuron; the third step is to correct the weight vectors of the winning neuron and its neighboring neurons. **Event triggering occurs in three situations, namely obstacles on the path, load exceeding the upper limit, or inability to plan the Dubins path from the AUV to the pre-allocated target point. The event triggered control functions u is given by (12), where u_1 is the workload related function by (13) and u_2 is the obstacles related function by (14). The event triggered re-assignment will be implemented in the SOM algorithm flow chart if $u = 0$. After all target points are reached by one specified AUV, task allocation is completed.**

$$u = u_1 \& u_2 \quad (12)$$

$$u_1 = \begin{cases} 0, & D_{kjl} = \infty \\ 1, & \text{others} \end{cases} \quad (13)$$

$$u_2 = \begin{cases} 0, & ob_w > d_{safety} \\ 1, & ob_w \leq d_{safety} \end{cases} \quad (14)$$

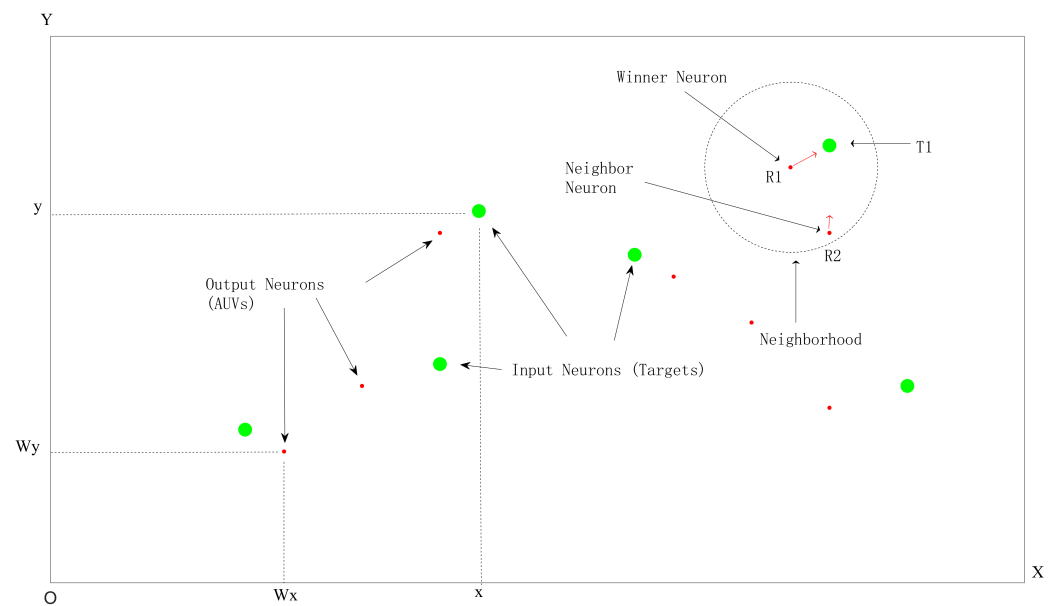


Figure 3. Schematic diagram of neighborhood weight change and load balance.

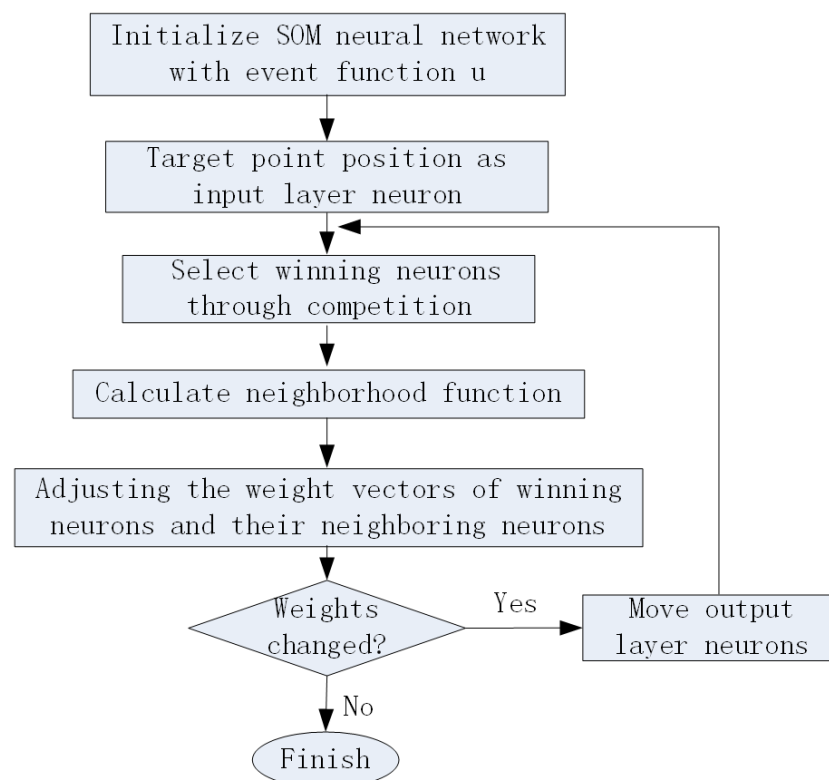


Figure 4. The event-triggered SOM algorithm flow chart.

2.2. Dubins path planning algorithm for AUV kinematic constraints

Unlike underwater robots such as ROVs, most torpedo like AUVs and underwater gliders are underactuated with tail thrusters to only moving forward, steering depend on fins and rudders. It is difficult to achieve proper path planning. Fortunately, Dubin's Car was introduced into the literature by Lester Dubins, a famous mathematician and statistician, in a paper published in 1957. The cars essentially have only 3 controls: "turn left at maximum", "turn right at maximum", and "go straight". All the paths traced out by the Dubin's car are combinations of these three controls. Dubin's car is very similar to AUVs'

kinematics. Assuming that the AUV has an initial velocity and dynamic characteristics as mentioned above, the path can be planned based on the Dubins car method from 2D to 3D workspace. Precise motion control to dynamic control problem is also very useful, which is another quite challenging field being studied. For example, command filter with adaptive control was proposed to solve the model uncertainties and input saturation issues [21]. These theories will be involved in our future work. To minimize the traveling time and energy consumption of AUVs, path planning based on kinematic is necessary. Here, we adopt the Dubins method to deal with the three-dimensional motion planning problem.

Literally, the Dubins curve is the shortest path connecting two points with initial directions, while satisfying curvature constraints and specified tangent lines (entry direction) at the beginning and end, and limiting the target to only turn forward. As described in prior works, the Dubins curve can be represented as a combination of three basic movements, as listed in Table 1. The Dubins curve provides a sufficient set of paths, which includes the optimal path. The shortest path is only selected from 6 curves in the set of LRL LSL LSR RLR RSR RSL.

Table 1. Table of concise classification of the Dubins path.

Symbol	Meaning	Direction
L	Turn left	Counterclockwise
R	Turn right	Clockwise
S	Go straight	Forward
C	Circular arc	Na
CCC	3 arcs	LRL RLR
CSC	2 arcs and 1 line segment	LSL RSR LSR RSL

Dubins curves in above table have been discussed in several papers such as [18] and [19], and related calculation methods are provided in former researches, which will not be repeated in this article. Two of the Dubin's shortest paths don't use the tangent lines. These are the RLR and LRL trajectories, which consist of three tangential, minimum radius turning circles [22,23]. These trajectories may be used very often in the swarm situation, where a lot of AUVs densely distributed in a certain 3D workspace. If the distance between the agent and the target's turning circles is less than 4 times the minimum turning radius r_{min} , then a CCC curve is valid. For CCC trajectories as an example, we must calculate the location of the third circle, as well as its tangent points to the circles. To be more concrete, the RLR case is shown in Figure 5.

Consider the minimum-radius turning circle to the right of start location to be the circle c_1 , and the minimum-radius turning circle to the right of the goal location to be the circle c_3 . The task is now to compute c_2 , a circle tangent to both c_1 and c_2 plus the points p_{t1} and p_{t2} which are respective points of intersection between the 3 circles. Let \mathbf{p}_1 , \mathbf{p}_2 , \mathbf{p}_3 be the centers of circle c_1 , c_2 , and c_3 , respectively. The triangle is formed using these points. Because c_2 is tangent to both c_1 and c_2 , the lengths of all three sides are known.

Segments $\overline{\mathbf{p}_1\mathbf{p}_2}$ and $\overline{\mathbf{p}_3\mathbf{p}_2}$ have length $2r_{min}$ and segment $\overline{\mathbf{p}_1\mathbf{p}_3}$ has length d . We are interested in the angle $\theta = \angle \mathbf{p}_3\mathbf{p}_1\mathbf{p}_2$ because that is the angle that the line between c_1 and c_3 (\vec{V}_1) must rotate to face the center of c_2 , which will allow us to calculate \mathbf{p}_2 by $\theta = \cos^{-1}\left(\frac{d}{4r_{min}}\right)$, where θ in a RLR trajectory represents the amount of rotation that vector $\vec{V}_1 = \mathbf{p}_3 - \mathbf{p}_1$ must rotate to point at the center of c_2 ; $d = \sqrt{(x_3 - x_1)^2 + (y_3 - y_1)^2}$. However, θ 's value is only valid if \vec{V}_1 is the same direction as the positive x-axis. Otherwise, the atan2 function will be needed to rotate \vec{V}_1 . For a LRL trajectory, we want to add θ to this value, but for an RLR trajectory we want to subtract θ from it to obtain a circle at the right-side of c_1 . Note that we consider counter-clockwise turns to be positive. Now that theta represents the absolute amount of rotation, we can compute the c_2 center point

$$\mathbf{p}_2 = (x_1 + 2r_{min}\cos(\theta), y_1 + 2r_{min}\sin(\theta)) \quad (15)$$

after which the tangent points p_{t1} and p_{t2} becomes easy to be computed. Defining vectors from the $\mathbf{p2}$ to $\mathbf{p1}$ and $\mathbf{p3}$, and walking down them a distance of r_{min} , we obtain the vector \vec{V}_2 from $\mathbf{p2}$ to $\mathbf{p1}$. Next, change the vector's magnitude to r_{min} by normalizing it and multiplying by r_{min}

$$\vec{V}_2 = \frac{\vec{V}_2}{\|\vec{V}_2\|} * r_{min} \quad (16)$$

where $\vec{V}_2 = \mathbf{p1} - \mathbf{p2}$. Next, compute p_{t1} using the new \vec{V}_2 by $p_{t1} = \mathbf{p2} + \vec{V}_2$. Then p_{t2} will be computed following a similar procedure.

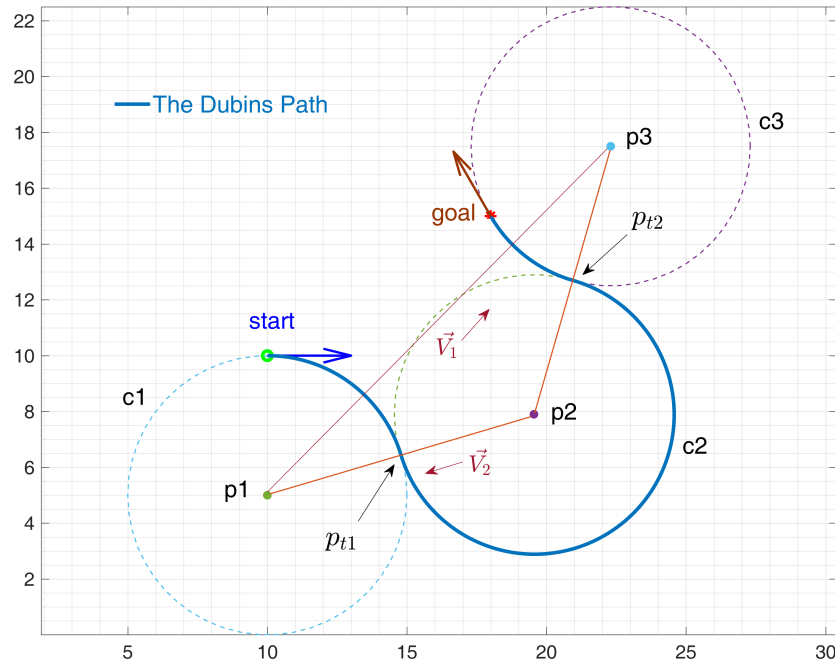


Figure 5. Computing a RLR Dubins trajectory.

As the tangent points are obtained, arc lengths and duration as before can be computed to finish things off. Then we get a Dubins path composed of 3 curves known as the CCC trajectory. To extend the 2D Dubins curves to 3D space using the linear interpolation method, the 3D tour sequences are first projected on to the 2D $[X, Y]$ plane in a global coordinate system. Taking a starting point $P_0(X_0, \Phi_0)$ and an ending point $P_1(X_1, \Phi_1)$ in the 3D $[X, Y, Z]$ space and project them on to the 2D plane. Then the starting and ending points become 2D parameters $[(x_0, y_0), \phi_0]$ and $[(x_1, y_1), \phi_1]$. The 2D Dubins curve is designed as described in the above content, and the lengths of the arcs and line segment are calculated. Let $\mathcal{L}_{0,x}$ and $\mathcal{L}_{x,1}$ denote the lengths along the 2D Dubins curve from (x_0, y_0) to (x, y) and from (x, y) to (x_1, y_1) , respectively. The linear interpolation adds the z coordinate in the 3D space by

$$z = z_0 + \frac{\mathcal{L}_{0,x}}{\mathcal{L}_{0,1}}(z_1 - z_0) \quad (17)$$

where z_0 and z_1 are the Z coordinates of the starting and ending points. Detailed procedure has been introduced in existing papers such as [17,20] and will not be repeated here. If obstacles appear in the path, we must re-assign the tasks.

After obtaining the dubins path, we modified the task allocation algorithm as following Figure 6. With kinematic constraints considered, the computing process increases base on algorithm 1. Due to the limited energy carried by autonomous underwater robots themselves, the rational and effective utilization of energy has become a key constraint for multi AUV systems to complete multiple tasks. Therefore, the load balancing of AUVs is considered in the algorithm. The paper assumes that AUVs carry the same energy, that

is, within the same working range, the distances traveled by AUVs exhausting their own energy are the same. Load balancing is determined by the traveling distance limit. At the same time, it is determined whether the distance between the winning AUV and the target task point meets the conditions for forming the Dubins Path. If not, it is set to infinity. Then the input neuron data could be modified in Algorithm 1 to reassign tasks to appropriate AUVs.

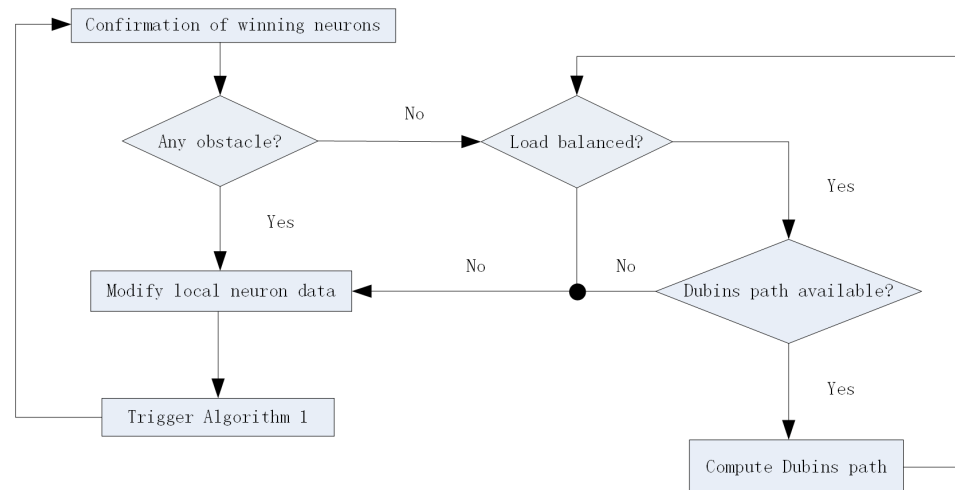


Figure 6. Flow chart of task assignment algorithm with Dubins path.

3. Simulation Research

Simulations were set up with multiple underwater targets deployed randomly in a work space of $[30 \times 30]$ units, where the minimum turning radius r_{min} of each AUV are the same and equal to 1 unit. Green dots represent targets, and red diamonds represent AUVs. In the workspace of a multi AUV system, there are 4 AUVs that need to access 6 randomly distributed targets. After the task is assigned by the SOM neural network, each AUV can reach its nearest target point along the optimal path, as shown in Figure 7. As there is no obstacle or load balance problem in this workspace, AUVs can accurately reach various target positions based on proposed algorithm.

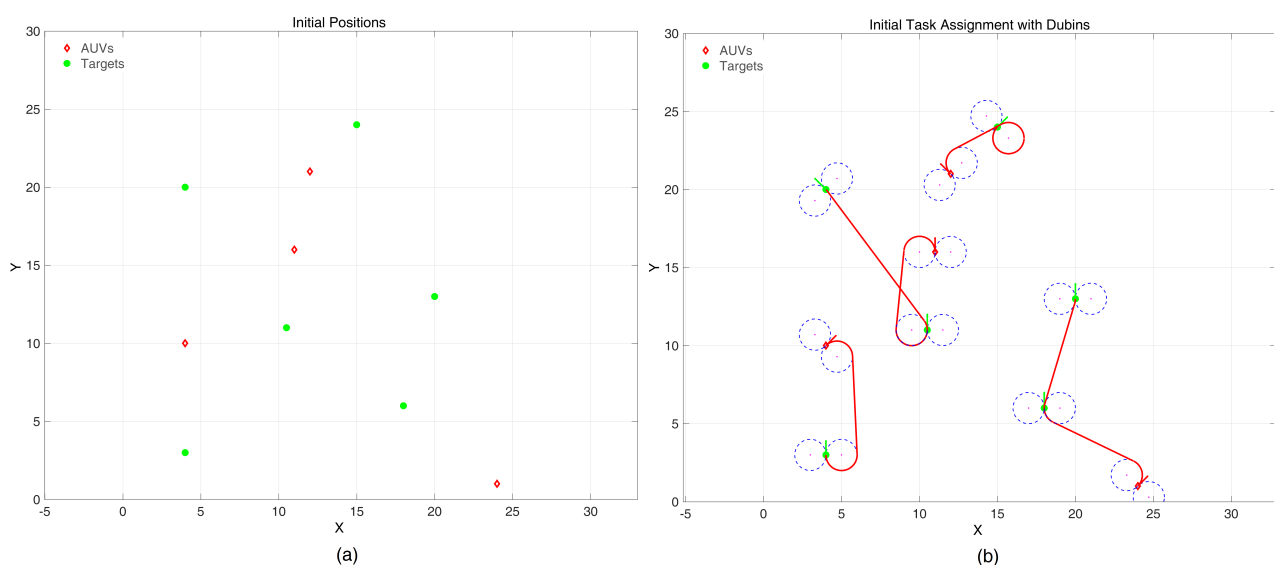


Figure 7. Task assignment in an initial obstacle free and load balance free environment.

In actual operation, there are often obstacles that affect the results of task allocation. We keep the positions of AUVs and target points unchanged, while add an obstacle area to the workspace, which may also affect the load balancing.

As Figure 8 illustrates, comparing Figure 8(b) to Figure 7(b), it can be found that when the route is blocked by the obstacle or the path cannot be planned, the current winning neuron is not selected, and the suboptimal neuron is used for route planning until the path planning is successful after the task re-assignment. All target points are also accessed by the closest distance. The simulation results prove that the algorithm is effective with obstacles.

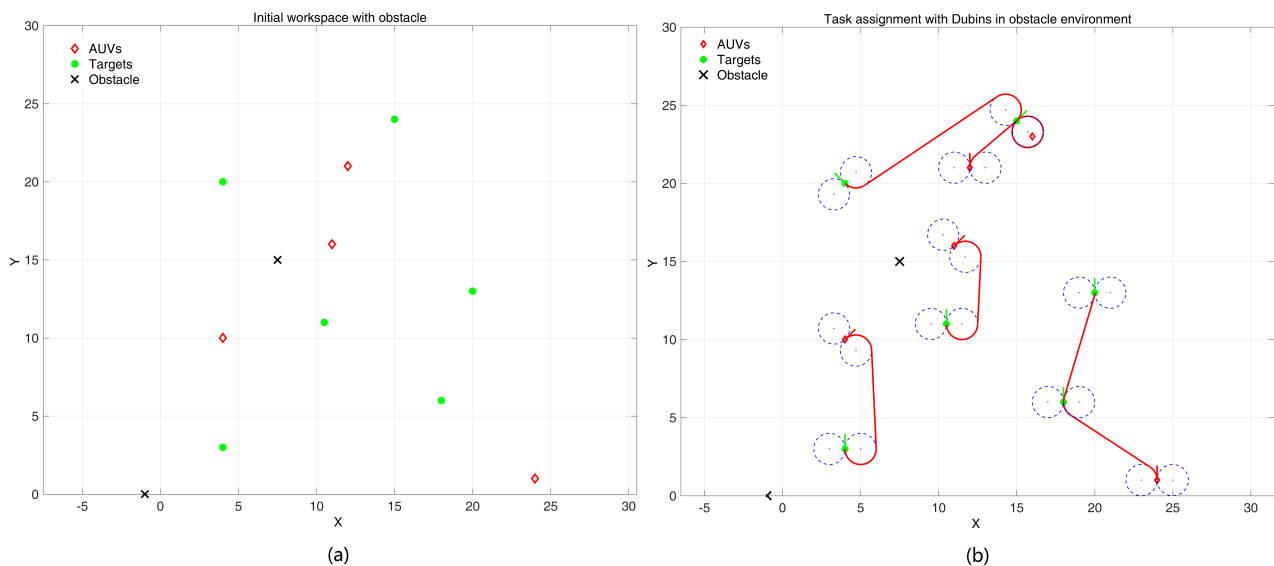


Figure 8. Task assignment and path planning in an obstacle environment.

In more cases, besides obstacles, there is also the issue of load balancing for AUVs. AUVs navigate in water and carry limited energy, which means the total range that a single AUV can navigate is limited. The algorithm proposed in this article can solve these problems within a certain range. The following is a simulation explanation.

As shown in Figure 9, in the workspace of a multi-AUV task assignment scenario, there are 2 AUVs that need to access 6 randomly distributed targets. Figure 9(a) shows task allocation and path planning without workload balance settings, where one AUV is responsible for four tasks and the other is responsible for two tasks. Figure 9(b) shows task allocation and path planning with a settings of number of task as 3. At this time, both AUVs are responsible for completing 3 tasks, and their energy consumption is relatively balanced. In the algorithm, the upper limit of task responsibility is set by default to the number of tasks divided by the number of robots, rounded up by 1. At the same time, the distance traveled is also recorded, and the maximum walking path upper limit is provided. When the upper limit is exceeded after the execution of this task, the task is not assigned to the winning robot. A series of tests are implemented as illustrated in Table 2. The path length is using "Unit" as a measurement unit as mentioned above.

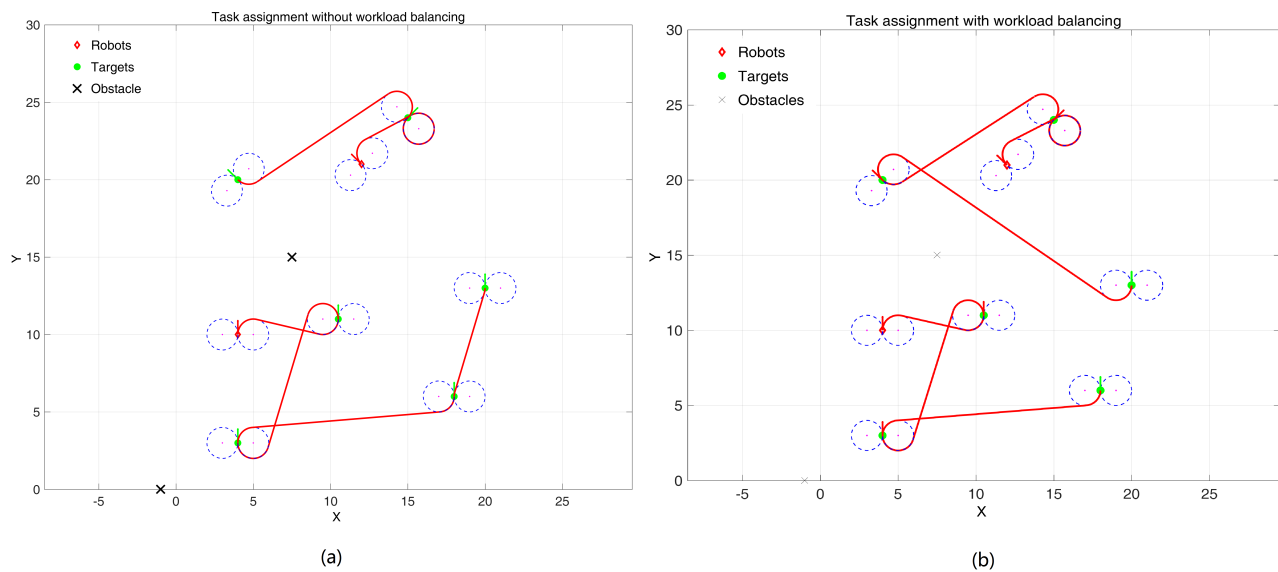


Figure 9. Task assignment in an obstacle environment with workload balancing.

Table 2. Task assignment and path planning results with and without workload balancing.

AUV Number (n)	Target Number	Whether Load Balanced	Path Length (Total)	Path Length (Max)	Tic Toc on PC (ms)	Clock on Pi (ms)
2	4	No	8.2	4.6	23	nul
	6	No	10.5	6.4	25	3550
	4	Yes	8.2	4.6	33	nul
	6	Yes	11.1	5.6	52	5012
4	6	No	10.6	3.0	30	nul
	8	No	15.2	5.7	32	nul
	6	Yes	11.5	2.2	51	nul
	8	Yes	16.1	4.1	55	nul
6	8	No	15.9	3.5	46	5276
	10	No	20.2	5.6	49	nul
	8	Yes	16.7	2.8	60	7189
	10	Yes	23.8	4.3	67	nul

As can be seen in the table above, the distance traveled by AUVs varies depending on whether load balancing is enabled or not. The algorithms were firstly implemented with MATLAB R2016a software on the hardware platform of HP Computer with Intel Core i7 9700 CPU and 16G DDR4 2400 memory. Simulation run time consumption was recorded using the Tic and Toc function. When there is no load balancing, the AUV obtains the minimum total distance based on the operation results of the SOM neural network, but the traveling length of a certain AUV may deviate from the average value. In the case of 4 AUVs for 8 targets, we calculate the mean square deviation of the distance based on the recorded running distance of each AUV, and the calculated formula is $\tilde{L} = \sqrt{\frac{\sum_{i=1}^n (L_i - \bar{L})^2}{n-1}}$. Then the standard deviation of the sample without load balancing can be obtained as 1.812; the standard deviation of the sample with load balancing can be obtained as 0.133. If there is no load balance, the load of a certain AUV may exceed the mean value significantly, which is not feasible in practical applications. Thus, we obtain the multi-task allocation results based on Dubins path planning under load balancing. Under load balancing, due to the fact that the pairing selection between certain AUVs and the target points may not be optimal in distance, the total path length will increase and the computation time will also

increase, which are all within an acceptable range on the level of tens of milliseconds. The simulation results show that the algorithm considering workload balance is effective.

Meanwhile, we implemented the algorithm through Python programs, with package NumPy. On the PC, the simulation time consumption with Python is approximately 5-10 times that of Matlab. In order to get closer to practical applications, we run Python simulations on the embedded device, an official Raspberry Pi 4B with 4G memory. The running times are shown in the table, which basically take a few seconds to complete the core algorithm, without drawing the graphics. Considering the rapid development of ARM computing power, it can be said feasible to run this algorithm on embedded systems. It should be noted that running on the Pi is only an experiment for the core program, not in an actual operation. The field applications may require an omniscient perspective and a known global map (or SLAM), which may involve various additional hardware.

Based on the method discussed in Section II, we extend the application to three-dimensional workspace. Task assignment and Dubins paths in 3D space also face obstacles and load balancing problems. Due to paper length limitations, we will provide an example of simulation here, without considering dynamic disturbances caused by water flow. Simulations were set up with multiple underwater targets deployed randomly in a 3D workspace, as shown in Figure 10(a). Note that in 3D environment the pitch angle γ is taken into algorithm and restricted to $[-15 * PI/180, 15 * PI/180]$. Task allocation result and trajectories are illustrated in Figure 10(b). We have simulated 30 Monte Carlo scenarios with AUVs and targets, and computed the average length of 3D trajectories. The standard deviation value \tilde{L} is relatively small since the proposed algorithms can achieve progressive optimization using load balancing scheme. The comparison results related to energy balance are shown in Table 3. We also implemented some simulations on PC (MATLAB) and Pi (Python). The average running time within an acceptable range has been recorded in the table.

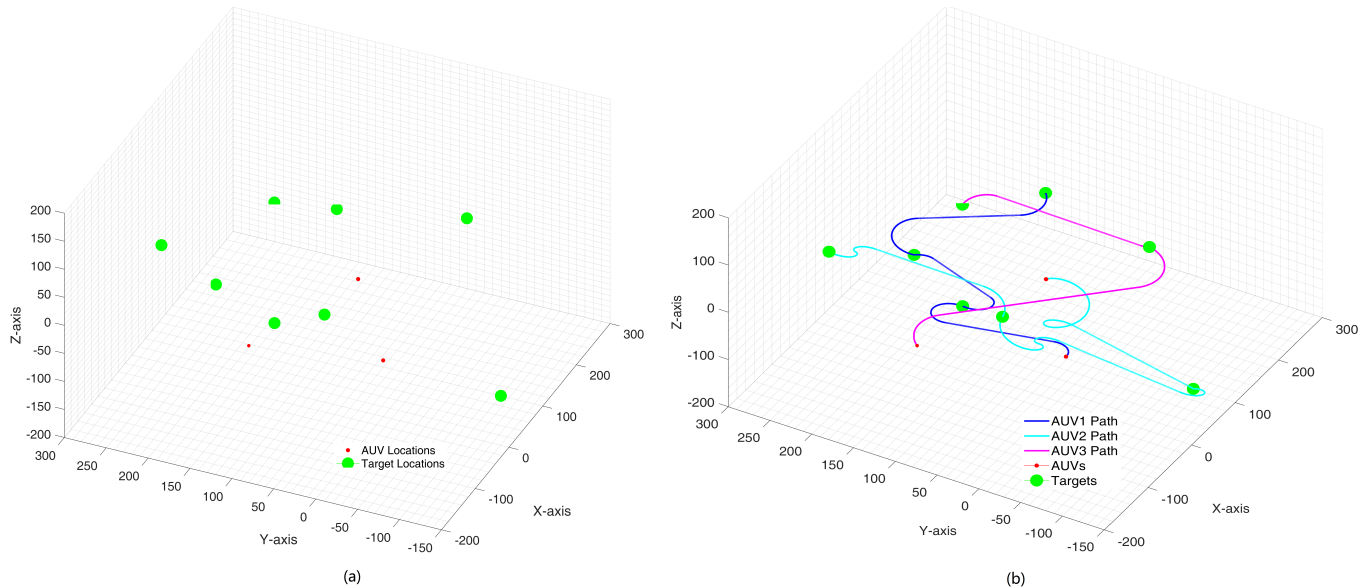


Figure 10. Task assignment in 3D environment with workload balancing.

Table 3. Task assignment and path planning results in 3D workspace with and without workload balancing.

AUV Number (<i>n</i>)	Target Number	Average Path Length	Standard Deviation (\bar{L})	Tic Toc on PC (ms)	Clock on Pi (ms)
3	8	103.5	1.005	78	8863
	10	131.7	0.516	81	nul
	15	206.0	0.232	101	nul
5	10	96.1	0.710	82	9012
	15	129.6	0.425	89	nul
	20	260.5	0.951	103	nul

4. Discussion and Future Work

This paper has studied the task assignment and path planning problem for multi-AUV systems with kinematic character considered. The improved SOM neural network method based on workload balance and neighborhood function is adopted to solve the strategy level issues for task allocation. Meanwhile, based on feasible kinematic path planning, combined with the Dubins method for path planning and task reassignment, task allocation and path planning under load balancing are finally achieved. **2D and 3D Dubins curves are designed with a set of possible headings and with nonholonomic motion constraints. It is demonstrated that the proposed method has been proven to achieve feasible load balancing for task assignment in obstacle environments. In future work, firstly, we will rewrite the algorithm in C++, hoping to achieve faster speed on embedded systems. Secondly, we will study more practical application and controllers related to dynamic control methods [24], such as Dubins trajectory tracking problem in water flow workspace of multi-AUV systems, as well as inter group collision avoidance of AUVs on the Dubins paths, and the moving obstacle avoidance problem.**

Acknowledgments: The authors would like to thank all the editors and reviewers who have given their valuable advice to this paper.

Conflicts of Interest: The authors declare no conflicts of interest.

References

- Gao, K.; Gao, M.; Zhou, M.; Ma, Z. Artificial intelligence algorithms in unmanned surface vessel task assignment and path planning: A survey. *SWARM AND EVOLUTIONARY COMPUTATION* **2024**, *86*. <https://doi.org/10.1016/j.swevo.2024.101505>.
- Oh, G.; Kim, Y.; Ahn, J.; Choi, H.L. Market-Based Task Assignment for Cooperative Timing Missions over Networks with Limited Connectivity. In Proceedings of the Aiaa Guidance, Navigation, & Control Conference, Aiaa Scitech, 2015.
- Cao, Z.H.; Bin, W.U.; Huang, Y.Q.; Deng, C.Y. The Multi-Robot Task Allocation Study Based on Improved Ant Colony Algorithm. *Modular Machine Tool & Automatic Manufacturing Technique* **2013**.
- Zhu, D.; Yang, S.X. Current Effect-Eliminated Optimal Target Assignment and Motion Planning for a Multi-UUV System. *IEEE Transactions on Intelligent Transportation Systems* **2024**, p. 1–10. <https://doi.org/10.1109/tits.2024.3351442>.
- Liu, S.; Sun, T.; Hung, C.C. *Multi-Robot Task Allocation Based on Swarm Intelligence*; Multi-Robot Systems, Trends and Development, 2011.
- Kohonen, T.K. Analysis of a simple self-organizing process. *Biological Cybernetics* **1982**.
- Zhao, C.; Guo, D. Particle Swarm Optimization Algorithm With Self-Organizing Mapping for Nash Equilibrium Strategy in Application of Multiobjective Optimization. *IEEE Transactions on Neural Networks and Learning Systems* **2020**, *PP*, 1–15.
- Zhu, A.; Yang, S. A Neural Network Approach to Dynamic Task Assignment of Multirobots. *IEEE Transactions on Neural Networks* **2006**, *17*, 1278–1287. <https://doi.org/10.1109/TNN.2006.875994>.
- Zhu, D.; Xin, L.; Mingzhong, Y. Task assignment algorithm of multi-AUV based on self-organizing map. *Control and Decision* **2012**, *27*, 1201–1204. <https://doi.org/10.13195/j.cd.2012.08.84.zhudq.030>.
- Li, X.; Zhu, D. An Adaptive SOM Neural Network Method for Distributed Formation Control of a Group of AUVs. *IEEE Transactions on Industrial Electronics* **2018**, *65*, 8260–8270. <https://doi.org/10.1109/TIE.2018.2807368>.
- Liu, J.; Wang, Q.G.; Yu, J. Event-Triggered Adaptive Neural Network Tracking Control for Uncertain Systems With Unknown Input Saturation Based on Command Filters. *IEEE Transactions on Neural Networks and Learning Systems* **2024**, *35*, 8702–8707. <https://doi.org/10.1109/TNNLS.2022.3224065>.

12. Jiang, K.; Seneviratne, L.D.; Earles, S. A Shortest Path Based Path Planning Algorithm for Nonholonomic Mobile Robots. *Journal of Intelligent & Robotic Systems* **1999**, *24*, 347–366.
13. Leng, J.; Liu, J.; Hongli, X.U. Online path planning of an unmanned surface vehicle for real-time collision avoidance. *CAAI Transactions on Intelligent Systems* **2015**.
14. Khatib, O. Real-Time Obstacle Avoidance System for Manipulators and Mobile Robots. *The International Journal of Robotics Research* **1986**, *5*, 90–98.
15. Sugihara, K. GA-based on-line path planning for SAUVIM. In Proceedings of the International Conference on Industrial & Engineering Applications of Artificial in Telligence & Expert Systems: Tasks & Methods in Applied Artificial Intelligence, 1998.
16. Li, T.; Chiang, M.S.; Jian, S.S. Motion planning of an autonomous mobile robot by integrating GAs and fuzzy logic control. In Proceedings of the IEEE IEEE International Conference on Fuzzy Systems, 2000.
17. Cai, W.; Zhang, M.; Zheng, Y. Task Assignment and Path Planning for Multiple Autonomous Underwater Vehicles Using 3D Dubins Curves. *Sensors* **2017**, *17*, 1607.
18. Lin, Y.; Saripalli, S. Path planning using 3D Dubins Curve for Unmanned Aerial Vehicles. In Proceedings of the 2014 International Conference on Unmanned Aircraft Systems (ICUAS), 2014.
19. Yu Wang.; Shuo Wang.; Min Tan.; Chao Zhou.; Qingping Wei. Real-Time Dynamic Dubins-Helix Method for 3-D Trajectory Smoothing. *IEEE Transactions on Control Systems Technology* **2015**, *23*, 730–736. <https://doi.org/10.1109/TCST.2014.2325904>.
20. Vana, P.; Alves Neto, A.; Faigl, J.; Macharet, D.G. Minimal 3D Dubins Path with Bounded Curvature and Pitch Angle. In Proceedings of the 2020 IEEE International Conference on Robotics and Automation (ICRA), Paris, France, 2020; pp. 8497–8503. <https://doi.org/10.1109/ICRA40945.2020.9197084>.
21. Liu, Y.; Liu, J.; Wang, Q.G.; Yu, J. Adaptive Command Filtered Backstepping Tracking Control for AUVs Considering Model Uncertainties and Input Saturation. *IEEE Transactions on Circuits and Systems II: Express Briefs* **2023**, *70*, 1475–1479. <https://doi.org/10.1109/TCSII.2022.3221082>.
22. Giese, A. A Comprehensive, Step-by-Step Tutorial on Computing Dubin’s Curves. <https://gieseanw.wordpress.com/2012/10/21/a-comprehensive-step-by-step-tutorial-to-computing-dubins-paths/>, 2012–2023.
23. Shkel, A.M.; Lumelsky, V. Classification of the Dubins set. *Robotics and Autonomous Systems* **2001**.
24. Li, Y.; Li, X.; Zhu, D.; Yang, S.X. Self-Competition Leader-Follower Multi-AUV Formation Control Based On Improved Pso Algorithm With Energy Consumption Allocation. *International Journal Of Robotics & Automation* **2022**, *37*, 288–301. <https://doi.org/10.2316/J.2022.206-0563>.

Disclaimer/Publisher’s Note: The statements, opinions and data contained in all publications are solely those of the individual author(s) and contributor(s) and not of MDPI and/or the editor(s). MDPI and/or the editor(s) disclaim responsibility for any injury to people or property resulting from any ideas, methods, instructions or products referred to in the content.